



## Numerical analysis of flow around bluff bodies with 4<sup>th</sup> and 2<sup>nd</sup> order compact formulations

Erman Aslan<sup>1</sup>, İlker İnan<sup>\*2</sup>, İlyas Kandemir<sup>3</sup>, Hasan Rıza Güven<sup>4</sup>

### ABSTRACT

In the present study, fourth-order compact formulation has been improved for Navier-Stokes (N-S) equations, which is expressed for two-dimensional, steady, incompressible flow problems. N-S equation system has been expressed with Stream Function-Vorticity Approach using Finite Difference Method (FDM) from the numerical methods. In order to test the functionality and applicability of the improved numerical formulation, a sample for submerged bluff bodies, flow problem around cylinder with square cross-section was chosen as a benchmark problem. As a result of applying improved numerical formulation with Gauss-Seidel Relaxation Method was used for this benchmark problem. The benchmark problem was also solved with second-order accuracy and obtained numerical results were compared with fourth-order accuracy numerical results. With the same Reynolds Number and the same free-stream velocity values, fourth-order numerical results are more convergent than second-order numerical results. Furthermore, in the flow field for considered benchmark problem, separation bubble length that consisted in the wake region is increased proportionally depending on the alteration of the Reynolds Number values.

**Keywords:** Stream Function-Vorticity Formulation, Flow Around Bluff Body, Steady State Flow, Incompressible Flow.

### 1. INTRODUCTION

Miscellaneous more sophisticated solution methods have been proposed for encountered different engineering problems in different disciplines. Such as in fluid mechanics, heat transfer, thermodynamics, physics etc. disciplines encountered various engineering problems could be solved analytical, numerical or empirical

solution methods. In these disciplines several more engineering problems could not solve via analytical solution methods due to the nonlinearity of partial differential equation system (PDES) [1-3]. Just because of this reason, numerical methods such as Finite Difference Method (FDM), Finite Volume Method (FVM), Finite Element Method (FEM), Spectral Methods, Boundary Element Method (BEM), Lattice Boltzmann Method (LBM) or Particle Methods have been used very

<sup>1</sup> Istanbul University, Faculty of Engineering, Mechanical Engineering Dept., Istanbul, Turkey- erman.aslan@istanbul.edu.tr

<sup>\*</sup> Corresponding Author

<sup>2</sup> Istanbul Kavram College of Higher Education, Machinery and Metal Technology Dept., Istanbul, Turkey/ilker.inan@kavram.edu.tr

<sup>3</sup> Gebze Technical University, Faculty of Engineering, Mechanical Engineering Dept., Kocaeli, Turkey- kandemir@gtu.edu.tr

<sup>4</sup> Istanbul University, Faculty of Engineering, Mechanical Engineering Dept., Istanbul, Turkey- -hrguven@istanbul.edu.tr

commonly to discretize the PDES belong to solutions of these engineering problems. These numerical methods gives us approximate results for the considered engineering problems [2, 3]. The main criteria's of selection the numerical methods are stable solution, converged solution and high-speed of convergence or less computational time. After applying one of these numerical methods which mentioned above, to the considered problem, discretized equations belong to the desired physical variables such as velocity, pressure, shear stress, stream function, vorticity, etc. can be obtained. These discretized equations can be expressed via one of the iterative numerical methods such as Newton-Raphson, Gauss-Jacobi Elimination, Gauss-Seidel, Gauss-Seidel Relaxation, Implicit and Explicit Euler, Alternating Direction Implicit Methods (ADIM) etc. to obtain the iteration equations of desired physical variables. The obtained iteration equations have been computed consecutively for determined iteration number or times to get solution results of desired physical variables in solution domain. In the present paper, each numerical solution step which mentioned above was applied to flow around a stationary square obstacle in two-dimensional flow field with steady, incompressible and no temperature gradient respectively. As it can be remembered, this flow problem was selected as a benchmark problem. This each numerical solution step was applied in developed numerical method with fourth-order compact formulation with nine grid points.

In the literature, it is possible to find numerous numerical approaches which have been applied to the flow problem around circular cylinder, square cylinder or any different bluff bodies. The flow past around bluff bodies, especially flow around circular and square cylinders, have been an attraction in all kinds of fluid mechanical investigations for many years. Particularly, the analysis of external flow around a square cylinder and circular cylinder is a reference model for miscellaneous engineering problems and engineering executions such as designing of a submarine, a cooling tower, a heat exchanger, an expansion tank, a boiler, a condenser, an evaporator, a tall building, a bridge, a chimney, a trash rack, etc. [4, 5]. In the literature it can be

found excellent assessments on these subjects were written by Fletcher [6], Williamson [7], Zdravkovich [8]. In contrast to the overwhelming number of publications on the flow past circular cylinders [9], the square counterpart has not been investigated to the same extent, although it plays a dominant role in many technical applications such as building aerodynamics [10, 20].

In Fluid Mechanics or Computational Fluid Dynamics (CFD) literature can be found numerous numerical studies for two-dimensional, steady, incompressible engineering flow problem's solutions. FDM, FVM, FEM, BEM, LBM, etc. numerical methods have been used in different numerical studies to discretize the PDES belong to this benchmark problem which is flow around square cylinder and for obtaining results have been applied iterative numerical methods as mentioned above [2, 9, 21, 22, 23]. For instance in Aydın and Çuhadaroğlu's [24] study has been considered the same benchmark problem but Explicit Euler Numerical Method has been applied. In Explicit Euler Method to discretize PDES are used FDM. In order to discretize PDES, central finite difference derivative formulas are considered due to dimension size and forward finite difference derivative formulas are considered due to time size. Also in Aydın and Çuhadaroğlu's [24] study, time dependent and time independent flow has been considered. In addition to this, in many various numerical studies are considered different engineering problems with the same numerical solution method as used in this study. For example in Erturk et al.'s [25] study has been considered the same numerical method as used in this study but this numerical method has been applied to lid driven cavity flow problem. As it seen from this numerical study the benchmark problem is different but applied numerical method same as this study.

Also, numerical studies of flow around different bluff bodies such as trapezoidal, triangular etc. can be found in the literature. In the case of a sharp-edged model geometries such as a square cross-section cylinder or trapezoidal geometry, where the separation points are fixed at the leading edges, physical flow properties were not changed relatively to the Reynolds Number [26]. Davis et al. have been investigated the bounded flow around square cylinders numerically for

comprehensive range of Reynolds Number with different blockage ratios values such as  $\beta=1/4$  and  $\beta=1/6$  [12]. The blockage ratio,  $B$ , is the ratio of the cross-stream projection of the square (edge length for a symmetric square) to the domain width. Benim et al. [27] and Chattopadhyay [28] studied flow around the triangular prism numerically in the laminar regime and turbulent regime, respectively.

This article has been constituted from Inan's MSc. thesis [29]. In this article, to solve the benchmark problem as mentioned above, FDM has been applied to discretize the PDES belong to the solution and from the iterative numerical methods Gauss-Seidel Relaxation (Successive Under/Over Relaxation) Method has been employed to obtain iteration equation belong to the desired physical variables such as stream function  $\psi$  and vorticity  $\omega$ . FDM is included finite difference derivative formulas, such as backward difference, central difference and forward difference derivative formulas. For considered benchmark problem, all the PDES has been discretized via central finite difference derivative formulas. In the present paper, a change of parameters has been made which replaces the velocity components with a stream function and a vorticity. Stream function-vorticity  $\psi$ - $\omega$  equations were discretized by using Taylor Series Expansion (TSE) via central finite difference derivative formulas. In the literature can be found many different numerical studies by using TSE via FDM. Erturk et al. [26], have been used fourth-order compact formulation with five grid points discretization via second-order central difference formulation to solve two-dimensional, steady, incompressible N-S equations. Mathematically it is impossible using five grid points with second-order accuracy central finite difference derivative formulas to obtain fourth-order compact formulation. In order to obtain fourth-order compact formulation it has been used nine different grid points. Therefore, this matter is a difference from the other numerical studies and this matter can be considered the uniqueness of this study. Also, cross derivatives are not used in fourth-order compact formulation, however, Erturk et al. [25], Erturk and Gökçöl [30] and Erturk [31] were included cross derivative terms while obtaining fourth-order compact formulation.

This is the second difference and significant matter from the other numerical studies.

The aim of the present study is to solve the steady, two-dimensional, incompressible N-S equations using fourth-order compact formulation and as a result to obtain iteration equations. Simultaneously, applying the iteration equations to the benchmark flow problem which flow around square cylinder for different free-stream velocities and different Reynolds Number values in  $341 \times 81$  grid structure. Finally, we will compare second-order and fourth-order compact formulations to each other.

## 1. NUMERICAL SOLUTION METHODOLOGY

### 1.1. Governing Equations of Fourth-Order Compact Formulation

In this numerical analysis, the flow is considered to be two-dimensional, steady and incompressible with constant properties neglect pressure gradients and neglect body forces. With regard to these assumptions, the conservation of mass and the conservation of momentum equation can be expressed in nondimensionalized form and in Cartesian coordinate system as follows:

$$\frac{\partial u}{\partial x} + \frac{\partial v}{\partial y} = 0 \quad (1)$$

$$\rho \left( u \frac{\partial u}{\partial x} + v \frac{\partial u}{\partial y} \right) = \mu \left( \frac{\partial^2 u}{\partial x^2} + \frac{\partial^2 u}{\partial y^2} \right) \quad (2)$$

$$\rho \left( u \frac{\partial v}{\partial x} + v \frac{\partial v}{\partial y} \right) = \mu \left( \frac{\partial^2 v}{\partial x^2} + \frac{\partial^2 v}{\partial y^2} \right) \quad (3)$$

The above equations ((1), (2) and (3)) representing the conservation of mass and momentum equations can be rewritten in terms of stream function-vorticity formulation. The vorticity is expressed as:

$$\omega = \frac{\partial v}{\partial x} - \frac{\partial u}{\partial y} \quad (4)$$

The stream function is expressed in such a way that the continuity equation is identically satisfied. Then we have,

$$u = \frac{\partial \psi}{\partial y}; v = -\frac{\partial \psi}{\partial x} \quad (5)$$

Instead of solving (1), (2) and (3) in terms of primitive variables, the equations are rewritten in terms of stream function and the vorticity defined in equation (4) and equation (5).

$$\frac{\partial^2 \psi}{\partial x^2} + \frac{\partial^2 \psi}{\partial y^2} = -\omega \quad (6)$$

$$u \frac{\partial \omega}{\partial x} + v \frac{\partial \omega}{\partial y} = \nu \left( \frac{\partial^2 \omega}{\partial x^2} + \frac{\partial^2 \omega}{\partial y^2} \right) \quad (7)$$

Equations (6) and (7) are known as the Poisson's Equation and the Vorticity Transport Equation, respectively. In addition equation (6) is named Stream Function Equation and equation (7) is entitled Vorticity Equation, respectively. In order to provide sustainability between the various studies in this area and also to guard against undesirable numerical overflows, it is often helpful to perform numerical investigations using nondimensional parameters. Physical quantities are made dimensionless by using representative quantities. The nondimensionalized forms of equations (6) and (7) are as follows:

$$\frac{\partial^2 \psi}{\partial x^2} + \frac{\partial^2 \psi}{\partial y^2} = -\omega \quad (8)$$

$$\frac{\partial \psi}{\partial y} \frac{\partial \omega}{\partial x} - \frac{\partial \psi}{\partial x} \frac{\partial \omega}{\partial y} = \frac{1}{Re} \left( \frac{\partial^2 \omega}{\partial x^2} + \frac{\partial^2 \omega}{\partial y^2} \right) \quad (9)$$

In order to transform from physical domain to computational domain, the grids are mapped onto orthogonal grids. Physical domain means that distance between sequential grid points are not equal ( $\Delta x \neq \Delta y$ ) in other words, nonhomogeneous grid structure as shown in Fig. 1. a. Also computational domain means that distance between sequential grid points are equal ( $\Delta \xi = \Delta \eta$ ) in other words, homogeneous grid structure or orthogonal equidistant grid structure as shown in Fig. 1. b. In Fig. 1. a and Fig. 1. b,  $K(x_1, y_1)$ ,  $L(x_1, y_2)$  and  $M(x_1, y_3)$  notations shows that any grid points in considered grid structure.

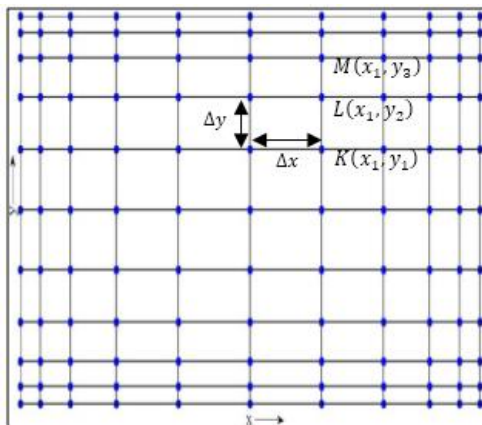


Figure 1. (a) Physical domain (Nonhomogeneous grid structure)

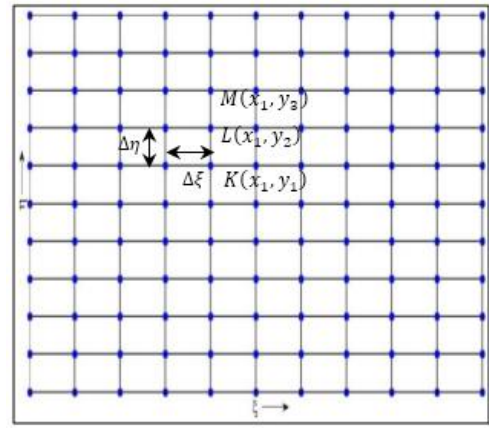


Figure 1. (b) Computational domain (Homogeneous grid structure)

Transform functions as shown below has been used to transform the above equations ((8) and (9)) in physical domain to computational domain. In the present paper, used transform functions are as follows [33]:

$$x = \xi - \frac{\lambda}{2\pi} (\sin(2\pi\xi)) \quad (10)$$

$$y = \eta - \frac{\lambda}{2\pi} (\sin(2\pi\eta)) \quad (11)$$

As a result of applying mathematical operations and requirements we will obtain the final form of the equations take the following form:

$$A \frac{\partial^2 \psi}{\partial \xi^2} + B \frac{\partial^2 \psi}{\partial \eta^2} + C \frac{\partial \psi}{\partial \xi} + D \frac{\partial \psi}{\partial \eta} = -\omega \quad (12)$$

$$\frac{1}{Re} \left( A \frac{\partial^2 \omega}{\partial \xi^2} + B \frac{\partial^2 \omega}{\partial \eta^2} + C \frac{\partial \omega}{\partial \xi} + D \frac{\partial \omega}{\partial \eta} \right) = E \left( \frac{\partial \psi}{\partial \eta} \frac{\partial \omega}{\partial \xi} - \frac{\partial \psi}{\partial \xi} \frac{\partial \omega}{\partial \eta} \right) \quad (13)$$

where  $A, B, C, D$  and  $E$  are the coefficients:

$$\begin{aligned} A &= \left( \left( \frac{\partial \xi}{\partial x} \right)^2 + \left( \frac{\partial \xi}{\partial y} \right)^2 \right) \\ B &= \left( \left( \frac{\partial \eta}{\partial x} \right)^2 + \left( \frac{\partial \eta}{\partial y} \right)^2 \right) \\ C &= \left( \frac{\partial^2 \xi}{\partial x^2} + \frac{\partial^2 \xi}{\partial y^2} \right) \\ D &= \left( \frac{\partial^2 \eta}{\partial x^2} + \frac{\partial^2 \eta}{\partial y^2} \right) \\ E &= \frac{\partial \xi}{\partial x} \frac{\partial \eta}{\partial y} \end{aligned} \quad (14)$$

The nondimensionalized N-S equations have been expressed above are nonlinear partial derivative differential equations and therefore need to be solved in an iterative manner. In the literature it can be found very different numerical methods to solve the partial differential equations, i.e., FVM, FEM, FDM, BEM and LBM. Among these methods, FDM is the oldest and is used to

discretize the nondimensional N-S equation system. In this method, the solution domain are divided to grid points (see in Fig. 1.b) and it is aimed to find the dependent variables only at that grid points. In FDM with TSE to obtain any order partial derivative expression three different approaches can be used such as forward finite difference, central finite difference and backward finite difference. In this study, to obtain finite difference equations, TSE with central difference approach has been used. The aim of using central difference approach is to obtain more accurate finite difference derivative formulas. In other words to obtain numerical solutions more closely to analytical results. Also fourth-order accuracy has been considered in central finite difference approach. The central finite difference derivative formulas with fourth-order accuracy has been tabulated in Table 1. The  $f$  is in Table 1 shows the general expression of any variable. In these central finite difference derivative formulas has been used twenty five different grid points, see in Fig. 2. In the present paper, central finite difference derivative formulas have been obtained with fourth-order accuracy and in the literature it cannot be found these formulas with fourth-order accuracy, except this paper.

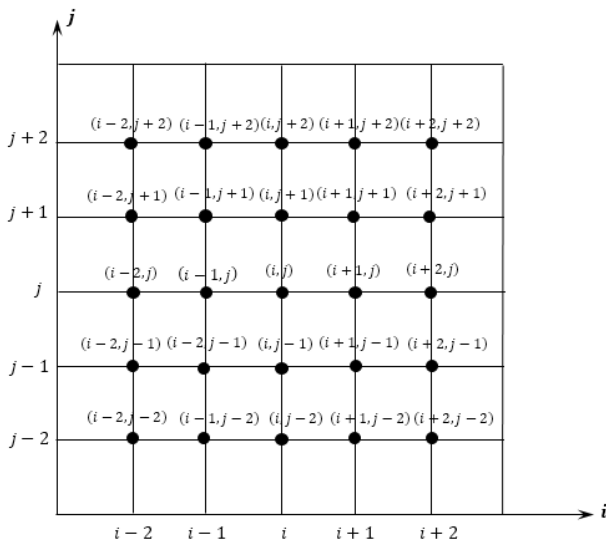


Figure 2. Used 25 different grid points at central finite derivative formulas with fourth-order accuracy

The Stream Function Equation is discretized using FDM with TSE and this equation can be expressed as follow:

$$A_{i,j} \left( \frac{-\psi_{i+2,j} + 16\psi_{i+1,j} - 30\psi_{i,j} + 16\psi_{i-1,j} - \psi_{i-2,j}}{12\Delta h^2} \right)$$

$$+ B_{i,j} \left( \frac{-\psi_{i,j+2} + 16\psi_{i,j+1} - 30\psi_{i,j} + 16\psi_{i,j-1} - \psi_{i,j-2}}{12\Delta h^2} \right) + C_{i,j} \left( \frac{-\psi_{i+2,j} + 8\psi_{i+1,j} - 8\psi_{i-1,j} + \psi_{i-2,j}}{12\Delta h} \right) + D_{i,j} \left( \frac{-\psi_{i,j+2} + 8\psi_{i,j+1} - 8\psi_{i,j-1} + \psi_{i,j-2}}{12\Delta h} \right) = -\omega_{i,j} \tag{15}$$

where  $A_{i,j}, B_{i,j}, C_{i,j}, D_{i,j}$  are the coefficients,  $\Delta h$  is difference between two sequential grid points,  $\psi_{i,j}$  is the stream function and  $\omega_{i,j}$  is the vorticity. Indices of  $(i, j)$  is denoted any grid points in grid structure, see in Fig. 2. In equation (15), it is not necessary to discretize  $A_{i,j}, B_{i,j}, C_{i,j}, D_{i,j}$  coefficients because these coefficients can be calculated algebraically. In equation (12),  $\frac{\partial \psi}{\partial \xi}, \frac{\partial \psi}{\partial \eta}$  are first-order and  $\frac{\partial^2 \psi}{\partial \xi^2}, \frac{\partial^2 \psi}{\partial \eta^2}$  are second-order partial derivative expressions. Equation (15) is discretized form of equation (12). Also, equation (12) is general expression of the stream function equation with fourth-order accuracy. At this stage, in order to obtain vorticity finite difference equation with fourth-order accuracy it has been applied the similar way and consequently the equation has been expressed as follow:

$$\frac{1}{Re} A_{i,j} \left[ \left( \frac{-\omega_{i+2,j} + 16\omega_{i+1,j} - 30\omega_{i,j} + 16\omega_{i-1,j} - \omega_{i-2,j}}{12\Delta h^2} \right) + B_{i,j} \left( \frac{-\omega_{i,j+2} + 16\omega_{i,j+1} - 30\omega_{i,j} + 16\omega_{i,j-1} - \omega_{i,j-2}}{12\Delta h^2} \right) + C_{i,j} \left( \frac{-\omega_{i+2,j} + 8\omega_{i+1,j} - 8\omega_{i-1,j} + \omega_{i-2,j}}{12\Delta h} \right) + D_{i,j} \left( \frac{-\omega_{i,j+2} + 8\omega_{i,j+1} - 8\omega_{i,j-1} + \omega_{i,j-2}}{12\Delta h} \right) \right] = E_{i,j} \left[ \left( \frac{-\psi_{i+2,j} + 8\psi_{i+1,j} - 8\psi_{i-1,j} + \psi_{i-2,j}}{12\Delta h} \right) \times \left( \frac{-\omega_{i+2,j} + 8\omega_{i+1,j} - 8\omega_{i-1,j} + \omega_{i-2,j}}{12\Delta h} \right) - \left( \frac{-\psi_{i+2,j} + 8\psi_{i+1,j} - 8\psi_{i-1,j} + \psi_{i-2,j}}{12\Delta h} \right) \times \left( \frac{-\omega_{i,j+2} + 8\omega_{i,j+1} - 8\omega_{i,j-1} + \omega_{i,j-2}}{12\Delta h} \right) \right] \tag{16}$$

In general expression of the stream function and the vorticity has been used nine different grid points, see in Fig. 3. These grid points were illustrated in Fig. 3.

In equation (13),  $\frac{\partial \omega}{\partial \xi}, \frac{\partial \omega}{\partial \eta}, \frac{\partial \psi}{\partial \xi}, \frac{\partial \psi}{\partial \eta}$  are first-order and  $\frac{\partial^2 \omega}{\partial \xi^2}, \frac{\partial^2 \omega}{\partial \eta^2}$  are second-order partial derivative expressions. Equation (16) is discretized form of equation (13). Also, equation (13) is general

expression of the vorticity equation with fourth-order accuracy.

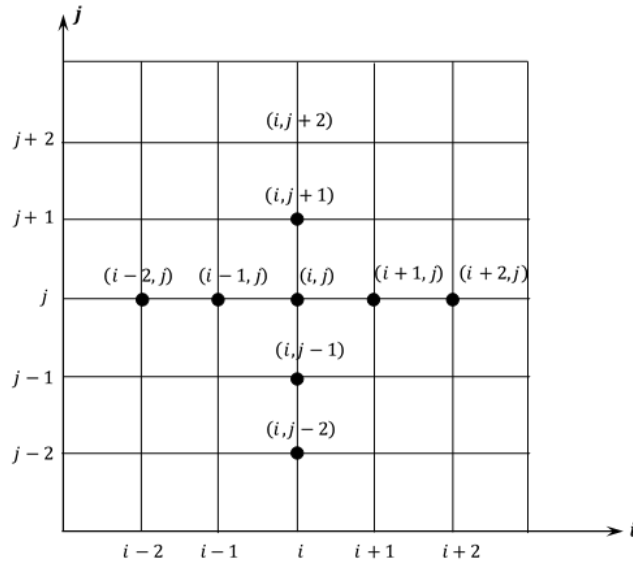


Figure 3. Used 9 different grid points at stream function and vorticity general expressions with fourth-order accuracy

Table 1. Central finite difference derivative formulas with fourth-order accuracy in Cartesian coordinate system

$\frac{\partial f}{\partial x} = \frac{-f_{i+2,j} + 8f_{i+1,j} - 8f_{i-1,j} + f_{i-2,j}}{12\Delta x} + \vartheta(\Delta x^4)$
$\frac{\partial f}{\partial y} = \frac{-f_{i,j+2} + 8f_{i,j+1} - 8f_{i,j-1} + f_{i,j-2}}{12\Delta y} + \vartheta(\Delta y^4)$
$\frac{\partial^2 f}{\partial x^2} = \frac{-f_{i+2,j} + 16f_{i+1,j} - 30f_{i,j} + 16f_{i-1,j} - f_{i-2,j}}{12\Delta x^2} + \vartheta(\Delta x^4)$
$\frac{\partial^2 f}{\partial y^2} = \frac{-f_{i,j+2} + 16f_{i,j+1} - 30f_{i,j} + 16f_{i,j-1} - f_{i,j-2}}{12\Delta y^2} + \vartheta(\Delta y^4)$
$\frac{\partial^2 f}{\partial x \partial y} = \left( \frac{f_{i+2,j+2} - 8f_{i+1,j+2} + 8f_{i-1,j+2} - f_{i-2,j+2} - 8f_{i+2,j+1} + 64f_{i+1,j+1} - 64f_{i-1,j+1} + 8f_{i-2,j+1}}{144\Delta x \Delta y} + \frac{8f_{i+2,j-1} - 64f_{i+1,j-1} + 64f_{i-1,j-1} - 8f_{i-2,j-1} - f_{i+2,j-2} + 8f_{i+1,j-2} - 8f_{i-1,j-2} + f_{i-2,j-2}}{144\Delta x \Delta y} \right) + \vartheta(\Delta x^4, \Delta y^4)$
$\frac{\partial^3 f}{\partial x^2 \partial y} = \left( \frac{f_{i+2,j+2} - 16f_{i+1,j+2} + 30f_{i,j+2} - 16f_{i-1,j+2} + f_{i-2,j+2} - 8f_{i+2,j+1} + 128f_{i+1,j+1} - 240f_{i,j+1} + 128f_{i-1,j+1} - 8f_{i-2,j+1}}{144\Delta x^2 \Delta y} + \frac{8f_{i+2,j-1} - 128f_{i+1,j-1} + 240f_{i,j-1} - 128f_{i-1,j-1} + 8f_{i-2,j-1} - f_{i+2,j-2} + 16f_{i+1,j-2} - 30f_{i,j-2} + 16f_{i-1,j-2} - f_{i-2,j-2}}{144\Delta x^2 \Delta y} \right) + \vartheta(\Delta x^4, \Delta y^4)$
$\frac{\partial^3 f}{\partial x \partial y^2} = \left( \frac{f_{i+2,j+2} - 16f_{i+2,j+1} + 30f_{i+2,j} - 16f_{i+2,j-1} + f_{i+2,j-2} - 8f_{i+1,j+2} + 128f_{i+1,j+1} - 240f_{i+1,j} + 128f_{i+1,j-1} - 8f_{i+1,j-2}}{144\Delta x \Delta y^2} + \frac{8f_{i-1,j+2} - 128f_{i-1,j+1} + 240f_{i-1,j} - 128f_{i-1,j-1} + 8f_{i-1,j-2} - f_{i-2,j+2} + 16f_{i-2,j+1} - 30f_{i-2,j} + 16f_{i-2,j-1} - f_{i-2,j-2}}{144\Delta x \Delta y^2} \right) + \vartheta(\Delta x^4, \Delta y^4)$
$\frac{\partial^4 f}{\partial x^2 \partial y^2} = \left( \frac{f_{i+2,j+2} - 16f_{i+1,j+2} + 30f_{i,j+2} - 16f_{i-1,j+2} + f_{i-2,j+2} - 16f_{i+2,j+1} + 256f_{i+1,j+1} - 480f_{i,j+1} + 256f_{i-1,j+1} - 16f_{i-2,j+1}}{144\Delta x^2 \Delta y^2} + \frac{30f_{i+2,j} - 480f_{i+1,j} + 900f_{i,j} - 480f_{i-1,j} + 30f_{i-2,j} - 16f_{i+2,j-1} + 256f_{i+1,j-1} - 480f_{i,j-1} + 256f_{i-1,j-1} - 16f_{i-2,j-1}}{144\Delta x^2 \Delta y^2} + \frac{f_{i+2,j-2} - 16f_{i+1,j-2} + 30f_{i,j-2} - 16f_{i-1,j-2} + f_{i-2,j-2}}{144\Delta x^2 \Delta y^2} \right) + \vartheta(\Delta x^4, \Delta y^4)$

## 1.2. Iteration Equations with Gauss-Seidel Relaxation Method of Nondimensionalized N-S Equation System

We will numerically solve both the N-S equations (8) and (9) and the introduced fourth-order compact formulation of the N-S equations (12) and (13). Both of these equation sets are nonlinear and therefore, they need to be solved in an iterative manner. In order to have an iterative numerical algorithm, we aimed to obtain an iteration equation of stream function, in the first solution stage. Gauss-Seidel Relaxation Method, with required mathematical operations and arrangements has been applied to obtain an iteration equation of the stream function. In addition the aim of applying Gauss-Seidel Relaxation Method is to solve the PDES in a short computation time via a computer programming code and to accelerate the convergence speed [1, 3, 29, 33]. To prevent the solution from the divergency, in other words to obtain much closer to analytical solution values it has been considered Gauss-Seidel Relaxation iterative numerical method. For this benchmark problem, as a result of applying iterative numerical method with required mathematical operations and arrangements it has been obtained an iteration equation of stream function with fourth-order accuracy as follow:

$$\begin{aligned} \psi_{i,j} = & w \left( \frac{1}{5(A_{i,j}+B_{i,j})} \right) \left[ - \left( \frac{\Delta h C_{i,j} + A_{i,j}}{6} \right) (\psi_{i+2,j}) \right. \\ & + \left( \frac{4(\Delta h C_{i,j} + 2A_{i,j})}{3} \right) (\psi_{i+1,j}) + \left( \frac{4(-\Delta h C_{i,j} + 2A_{i,j})}{3} \right) (\psi_{i-1,j}) \\ & + \left( \frac{\Delta h C_{i,j} - A_{i,j}}{6} \right) (\psi_{i-2,j}) - \left( \frac{\Delta h D_{i,j} + B_{i,j}}{6} \right) (\psi_{i,j+2}) \quad (17) \\ & + \left( \frac{4(\Delta h D_{i,j} + 2B_{i,j})}{3} \right) (\psi_{i,j+1}) + \left( \frac{4(-\Delta h D_{i,j} + 2B_{i,j})}{3} \right) (\psi_{i,j-1}) \\ & + \left( \frac{\Delta h D_{i,j} - B_{i,j}}{6} \right) (\psi_{i,j-2}) + (2\Delta h^2)(\omega_{i,j}) \\ & \left. + (1-w)\psi_{i,j} \right] \end{aligned}$$

where  $w$  is the relaxation parameter. Relaxation parameter refers to convergence speed in Successive Under Relaxation Method. Also, relaxation parameter changes from 0.0 to 1.0 for under relaxation.

In the second solution stage, for obtaining an iteration equation of the vorticity, it can be followed the same way with the stream function.

$$\begin{aligned} \omega_{i,j} = & w \left( \frac{1}{15(A_{i,j}+B_{i,j})} \right) \left[ - \left( \frac{\Delta h C_{i,j} + A_{i,j}}{2} \right) (\omega_{i+2,j}) \right. \\ & + (4\Delta h C_{i,j} + 8A_{i,j})(\omega_{i+1,j}) + (-4\Delta h C_{i,j} + 8A_{i,j})(\omega_{i-1,j}) \\ & + \left( \frac{\Delta h C_{i,j} - A_{i,j}}{2} \right) (\omega_{i-2,j}) - \left( \frac{\Delta h D_{i,j} + B_{i,j}}{2} \right) (\omega_{i,j+2}) \\ & + (4\Delta h D_{i,j} + 8B_{i,j})(\omega_{i,j+1}) + (-4\Delta h D_{i,j} + 8B_{i,j})(\omega_{i,j-1}) + \left( \frac{\Delta h D_{i,j} - B_{i,j}}{2} \right) (\omega_{i,j-2}) \\ & - \frac{Re}{24} E_{i,j} (-\psi_{i,j+2} + \psi_{i,j-2})(-\omega_{i+2,j} + \omega_{i-2,j}) \\ & - \frac{Re}{3} E_{i,j} (-\psi_{i,j+2} + \psi_{i,j-2})(\omega_{i+1,j} - \omega_{i-1,j}) \\ & - \frac{Re}{3} E_{i,j} (\psi_{i,j+1} - \psi_{i,j-1})(-\omega_{i+2,j} + \omega_{i-2,j}) \\ & - \frac{8Re}{3} E_{i,j} (\psi_{i,j+1} - \psi_{i,j-1})(\omega_{i+1,j} - \omega_{i-1,j}) \quad (18) \\ & + \frac{Re}{24} E_{i,j} (-\psi_{i+2,j} + \psi_{i-2,j})(-\omega_{i,j+2} + \omega_{i,j-2}) \\ & + \frac{Re}{3} E_{i,j} (-\psi_{i+2,j} + \psi_{i-2,j})(\omega_{i,j+1} - \omega_{i,j-1}) \\ & + \frac{Re}{3} E_{i,j} (\psi_{i+1,j} - \psi_{i-1,j})(-\omega_{i,j+2} + \omega_{i,j-2}) \\ & \left. + \frac{8Re}{3} E_{i,j} (\psi_{i+1,j} - \psi_{i-1,j})(\omega_{i,j+1} - \omega_{i,j-1}) \right] + (1-w)\omega_{i,j} \end{aligned}$$

Consequently, to compute stream function and vorticity values with fourth-order accuracy in any grid points and with iterative manner, can be used iteration equation (17) and (18), respectively.

## 1.3. Comparison Between Second-Order Accurate and Fourth-Order Accurate Compact Formulation

Nondimensionalized N-S equation system (equation (8) and (9)) has been solved numerically via fourth-order accurate compact formulation. While obtaining iteration equation with fourth-order accuracy, it has been used 9 different grid points as mentioned before. In addition to solve nondimensionalized N-S equation system, second-order accurate compact formulation with Gauss-Seidel Relaxation Method are used. The stream function and the vorticity equation is shown in equation (19) and (20), respectively.

$$\begin{aligned} \psi_{i,j} &= w \left( \frac{1}{2(A_{i,j}+B_{i,j})} \right) \left[ (A_{i,j} + \frac{\Delta h}{2} C_{i,j}) \psi_{i+1,j} \right. \\ &+ (A_{i,j} - \frac{\Delta h}{2} C_{i,j}) \psi_{i-1,j} + (B_{i,j} + \frac{\Delta h}{2} D_{i,j}) \psi_{i,j+1} \\ &\left. + (B_{i,j} - \frac{\Delta h}{2} D_{i,j}) \psi_{i,j-1} + \Delta h^2 (\omega_{i,j}) \right] + (1-w) \psi_{i,j} \quad (19) \\ \omega_{i,j} &= w \left( \frac{1}{2(A_{i,j}+B_{i,j})} \right) \left[ (A_{i,j} + \frac{\Delta h}{2} C_{i,j}) \omega_{i+1,j} \right. \\ &+ (A_{i,j} - \frac{\Delta h}{2} C_{i,j}) \omega_{i-1,j} + (B_{i,j} + \frac{\Delta h}{2} D_{i,j}) \omega_{i,j+1} \\ &+ (B_{i,j} - \frac{\Delta h}{2} D_{i,j}) \omega_{i,j-1} \\ &- \frac{Re}{4} E_{i,j} (\psi_{i,j+1} - \psi_{i,j-1}) (\omega_{i+1,j} - \omega_{i-1,j}) \\ &\left. + \frac{Re}{4} E_{i,j} (\psi_{i+1,j} - \psi_{i-1,j}) (\omega_{i,j+1} - \omega_{i,j-1}) \right] \\ &+ (1-w) \omega_{i,j} \quad (20) \end{aligned}$$

In order to compute stream function values with second-order accuracy in any grid points it can be used iteration equation (19). In a similar fashion to compute vorticity values with fourth-order accuracy in any grid points it can be used iteration equation (20). Equation (19) and (20) have been used 5 different grid points such as  $(i + 1, j)$ ,  $(i, j)$ ,  $(i - 1, j)$ ,  $(i, j + 1)$  and  $(i, j - 1)$ , see in Fig. 3. In second-order compact formulation has been considered less grid points than fourth-order compact formulation.

We generate the in-house FDM code. In this in-house FDM code, fourth and second-order compact formulation are used to compute stream function and vorticity values. It is observed that computing time of second-order compact formulation less than computing time of fourth-order compact formulation.

### 3. PROBLEM DEFINITION

In the present paper, the obtained second-order and fourth-order compact formulations with Gauss-Seidel Relaxation Method have been applied to flow around a square cylinder as selected a benchmark problem. Numerical values in two-dimensional flow field have been obtained in  $341 \times 81$  grid points. Square cylinder has been positioned in free-stream area and between top and bottom free boundaries. This square cylinder has been considered as an immersed body. Flow around a square cylinder has been illustrated in Fig. 4. Around the square cylinder existing

Newtonian fluid which is shear stress ratio changes linearly with rate of strain.

### 3.1. Boundary Conditions in Flow Around Square Cylinder Problem

In this benchmark problem, left and right boundaries are input and output boundaries, respectively. These boundaries are free boundaries. In other words, these boundaries are not a wall. In a similar fashion, top and bottom boundaries are free boundaries. Considered velocity components in  $x$ -direction  $u$  values, in  $y$ -direction  $v$  values and distance between square cylinder and free boundaries has been illustrated in Fig. 4. In free-stream area, considered velocity boundaries have been tabulated in Table 2.

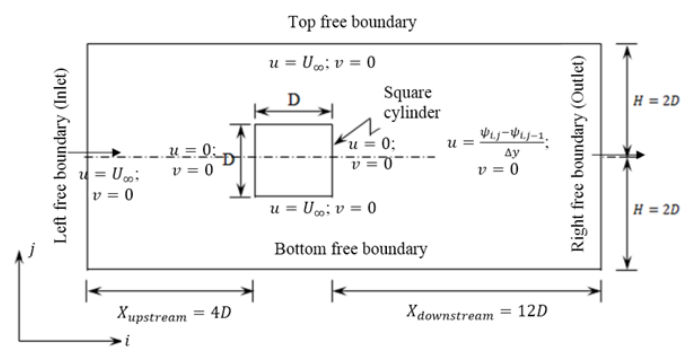


Figure 4. Schematic view of flow around square cylinder problem and computational domain and boundary conditions

Table 2. Considered boundary conditions in free-stream area.

Bottom and top, free boundaries	:	$u = U_{\infty}; v = 0$
Left, free boundary	:	$u = U_{\infty}; v = 0$
Right, free boundary	:	$u = \frac{\psi_{i,j} - \psi_{i,j-1}}{\Delta y}; v = 0$
Square cylinder, no-slip boundary condition	:	$u = 0; v = 0$

In two-dimensional flow area, square cylinder are considered as stationary wall. Due to this reason, no-slip boundary conditions are used at the edges on square cylinder. For the no-slip boundary conditions, velocity components in  $x$ -direction  $u$  values and in  $y$ -direction  $v$  values are equal to zero therefore stream function values are also equal to zero. However vorticity values are nonzero. In the literature it can be found different methods to compute vorticity values such as Stortkuhl Method, Thom's Method, etc. In this study, in order to compute vorticity values in grid structure

it has been used Thom's Method. The no-slip boundary conditions at square cylinders are converted for stream function and vorticity approaches. The diverted no-slip boundary conditions have been demonstrated in Fig. 5.

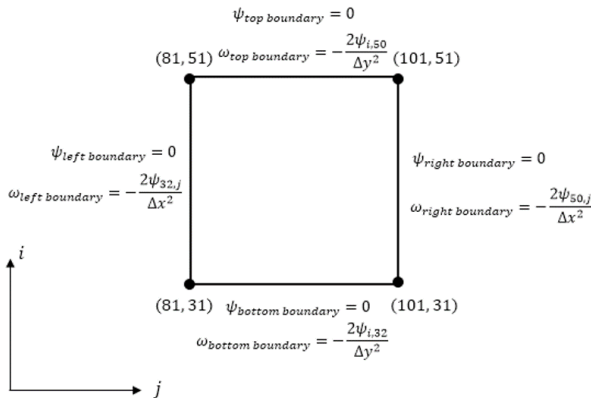


Figure 5. Equations of stream function and vorticity values on boundaries of square cylinder

For solving this benchmark problem,  $341 \times 81$  grid size is used. In these grid points it has been computed stream function and vorticity values. Constituted homogenous grid structure with  $341 \times 81$  grid size is showed in Fig. 6.

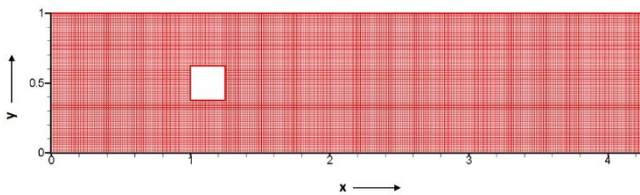


Figure 6. Homogeneous grid structure with  $341 \times 81$  grid size using in flow around square cylinder problem.

In numerical study, five different Reynolds numbers are used which are  $Re = 100$ ,  $Re = 300$ ,  $Re = 1000$ ,  $Re = 10000$  and  $Re = 20000$ . Reynolds number is based on free-stream velocity  $U_\infty$ , height of square  $D$  and kinematic viscosity  $\nu$ . For acquiring each Reynolds numbers, fifteen different free-stream velocities are taken which are  $U_\infty = 0.02$ ,  $U_\infty = 0.04$ ,  $U_\infty = 0.046$ ,  $U_\infty = 0.07$ ,  $U_\infty = 0.09$ ,  $U_\infty = 0.093$ ,  $U_\infty = 0.7$ ,  $U_\infty = 0.9$ ,  $U_\infty = 0.93$ ,  $U_\infty = 1.0$ ,  $U_\infty = 2.0$ ,  $U_\infty = 2.29$ ,  $U_\infty = 7.0$ ,  $U_\infty = 9.0$  and  $U_\infty = 9.3$ . Therefore, seventy five different cases are constituted. Additionally, the relaxation parameter and grid stretching parameter are kept as 0.01 and 0.05, respectively.

#### 4. RESULTS AND DISCUSSIONS

In order to compute whole stream function and vorticity values in  $341 \times 81$  grid structure, it has

been used stream function and vorticity iteration equations with fourth-order and second-order accuracy. A computer programming code has been constituted via the language of technical computing programming MATLAB R2010a [34]. The programming code has been run for five different Reynolds numbers and fifteen different free-stream velocities, therefore seventy five Reynolds number and free-stream velocity pairs are considered for each order accuracies which are fourth-order and second-order accuracy.

For fourth-order accuracy iterative numerical solution, thirty different Reynolds number and free-stream velocity pairs could not be solved, see in Table 3. Thirty eight Reynolds number and free-stream velocity pairs could be produced undefined values of stream function and vorticity parameters, for second-order accuracy iterative numerical solution, see in Table 4. In fourth-order accuracy iterative numerical solution, more Reynolds number and free-stream velocity pairs are solved than second-order accuracy iterative numerical solution, because of increasing of accuracy. Our problem is solved as a steady-state, however at high Reynolds numbers, the problem physics goes to unsteady. Therefore, at high Reynolds numbers, solvable free-stream velocity interval is small.

##### 4.1. Preliminary Validation

For the comparison of our in-house FDM code, FVM based commercial multi-purpose CFD code Ansys Fluent [35] is used. In comparison study, the same benchmark problem which is flow around square cylinder is used at  $Re = 40$  with the same free-stream velocity  $U_\infty = 1.0$ . Problem is assumed incompressible, two-dimensional and steady-state. The same grid size ( $341 \times 81$ ) is applied for the comparisons. Two comparison studies are used for preliminary validation. First comparison is made between in-house finite difference code with fourth-order compact formulation and FVM-based commercial CFD code Ansys-Fluent [35]. Second comparison is made at in-house Finite difference code between 2<sup>nd</sup> and 4<sup>th</sup> order compact formulations.

Fig. 7 shows the predicted streamlines for the first comparison which is between and FVM based commercial CFD code Ansys-Fluent [35] (Fig. 7.a) and in-house FDM code with fourth-order compact formulation (Fig. 7.b). In Fig. 7, the

nondimensional stream function has the value “-1” on the lower symmetry and the value “1” on the upper symmetry, where the step size between streamlines is 0.004. After the square cylinder, recirculation zone is consist for both numerical simulations. One can see in Fig. 7, recirculation zone length is same for both numerical calculations, and circulation length is approximately one edge length of square  $D$ . Therefore, our in-house FDM code with fourth-order compact formulation is validated.

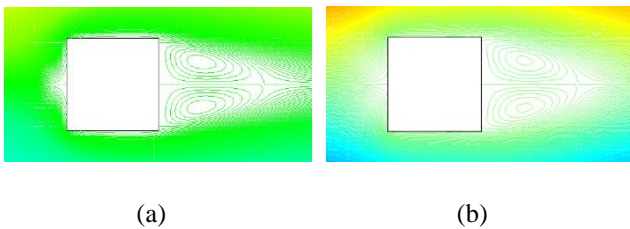


Figure 7. Streamlines at  $Re = 40$

- (a) for FVM based commercial CFD code Ansys-Fluent  
(b) for in-house FDM code with fourth-order compact formulation

The predicted streamlines from in-house FDM code second-order compact formulation (Fig. 8. a) and fourth-order compact formulation (Fig. 8. b) is shown at Fig. 8. Both numerical simulations are similar to each other. It means, in this Reynolds number, second and fourth-order compact formulations produce the same result. Therefore, second-order compact formulation of FDM is validated too.

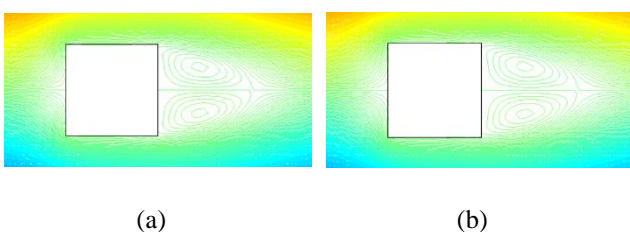


Figure 8. Streamlines at  $Re = 40$

- (a) for Finite Difference in-house code with second-order compact formulation  
(b) for Finite Difference in-house code with fourth-order compact formulation

#### 4.1. Main Benchmark Problem

Table 3 and 4 shows the numerical values stream function and vorticity with regard to different Reynolds number and different free-stream velocities for fourth-order and second-order compact formulations, respectively. As mentioned

before, seventy five Reynolds number and free-stream velocity pairs are taken into account. Forty five different Reynolds number and free-stream velocity pairs could be solved for fourth-order accuracy iterative numerical solution (Table 3). However, number of solvable Reynolds number and free-stream velocity pairs is thirty seven for second-order accuracy iterative numerical solution (Table 4). For both iterative numerical solution, solvable free-stream velocity values interval is large at low Reynolds numbers. With increasing Reynolds number, only small free-stream velocity values could be solved. It means, solvable free-stream velocity values interval is small at high Reynolds numbers. We assumed that our problem is steady-state, but, the problem physics go unsteady at high Reynolds number, thus, solvable free-stream velocity interval is small. Maximum and minimum stream function values are occurred positive and negative to half of free-stream velocity values, respectively. The difference maximum between minimum stream function values gives us a free-stream velocity values, because of mass conservation. Therefore, with increasing free-stream velocity values, difference maximum between minimum stream function values increase regardless to Reynolds number. Also, vorticity values are produced in-house FDM code. If absolute value is taken from minimum vorticity values, minimum vorticity value is equal to maximum vorticity value, like stream function values for both iterative numerical formulation. With increasing Reynolds number or free-stream velocity values, interval of vorticity which is difference between maximum and minimum vorticity, increases. One can see in Table 3 and 4, at the same Reynolds number and free-stream velocity values, fourth-order numerical formulations produce higher vorticity intervals than second-order numerical formulation.

Stream function contour graphics regarding different Reynolds numbers and 0.02 free-stream velocity value are presented in Table 5 for fourth-order numerical formulation and in Table 6 for second-order numerical formulation. All the figures in Table 5 and 6, nondimensional stream function has the value “-1” on the lower symmetry and the value “1” on the upper symmetry, where the step size between streamlines is 0.01, for better visualization and

comparison. The recirculation is observed after square cylinder especially at high Reynolds numbers because of negative velocity values. One can see in Table 5 and Table 6, recirculation zone length after square cylinder increases with increasing Reynolds number. Free-stream values are not a function of recirculation zone length, in other words, at the same Reynolds number, recirculation zone length does not change with free-stream velocities. The von Karman vortex streets after square cylinder are not observed because of using of steady state assumption, again. If the unsteady assumption is used in-house FDM code, von Karman vortex streets after square cylinder can be observed. For all solvable Reynolds number and free-stream pairs, second-order numerical formulation is produced a little bit higher recirculation zone length than fourth-order numerical formulation at corresponding Reynolds number. Therefore, fourth-order numerical formulations gives more realistic and accurate results than second-order numerical formulation.

## 5. CONCLUSIONS

The second-order and fourth-order compact formulation with Gauss-Seidel Relaxation Method have been applied to flow around a square cylinder, with two-dimensional and steady state assumptions. In numerical simulation, in-house FMD code is generated using MATLAB R2010a programming language [34].  $(341 \times 81)$  grid size is used for numerical calculations. Seventy five Reynolds number and velocity pairs are calculated for five different Reynolds number and fifteen different free-stream velocities. According to these numerical calculations, the following major conclusions are deduced;

- Nine different grid points are taken into account to obtain fourth-order compact formulation, because contributions of cross derivative terms, go to zero.
- Various Reynolds number and free-stream velocities are solved in fourth-order numerical formulation.
- With increasing Reynolds number, converged free-stream velocity values are decreased. At high Reynolds Numbers,

small free-stream values can be solved with fourth and second-order numerical formulations.

- Stream function that corresponds to free-stream centerline is considered as zero. Because of conservation of mass, if free-stream velocity increases, the stream function interval increases.
- The absolute values of minimum and maximum vorticities are equal, like stream function. With increasing Reynolds number, interval of vorticity increases. Fourth-order numerical formulation produces higher vorticity intervals than second-order numerical formulation.
- Length of recirculation zone increases with increasing Reynolds number values. Recirculation zone length does not depended on free-stream velocities.
- Von Karman streets are not observed because of the steady state assumption. This phenomena is unphysical in many cases.
- Second-order numerical formulation produced a little bit higher recirculation zone length than fourth-order numerical formulation at corresponding Reynolds numbers.
- Second-order numerical formulation gives less realistic and accurate results than fourth-order numerical formulation.

Table 3. Fourth-Order Numerical Values of Stream Function and Vorticity regarding Different Reynolds Numbers and Different Free Stream Velocity Values

Free-stream Velocity Values ( $U_\infty$ [m/s])	Reynolds Number ( $Re$ ) Values				
	100	300	1000	10000	20000
0.02	$\psi_{min.} = -0.01; \psi_{max.} = 0.01$             $\psi_{min.} = -0.01; \psi_{max.} = 0.01$				
	$\omega_{min.} = -1.1303; \omega_{max.} = 1.1303$	$\omega_{min.} = -1.2173; \omega_{max.} = 1.2173$	$\omega_{min.} = -1.5292; \omega_{max.} = 1.5292$	$\omega_{min.} = -2.61; \omega_{max.} = 2.61$	$\omega_{min.} = -2.5579; \omega_{max.} = 2.5579$
0.04	$\psi_{min.} = -0.02; \psi_{max.} = 0.02$             $\psi_{min.} = -0.02; \psi_{max.} = 0.02$				
	$\omega_{min.} = -2.3465; \omega_{max.} = 2.3465$	$\omega_{min.} = -2.7059; \omega_{max.} = 2.7059$	$\omega_{min.} = -3.7724; \omega_{max.} = 3.7724$	$\omega_{min.} = -5.1157; \omega_{max.} = 5.1157$	$\omega_{min.} = -4.7026; \omega_{max.} = 4.7026$
0.046	$\psi_{min.} = -0.023; \psi_{max.} = 0.023$           $\psi_{min.} = -0.023; \psi_{max.} = 0.023$				
	$\omega_{min.} = -2.7286; \omega_{max.} = 2.7286$	$\omega_{min.} = -3.2052; \omega_{max.} = 3.2052$	$\omega_{min.} = -4.5284; \omega_{max.} = 4.5284$	$\omega_{min.} = -5.81; \omega_{max.} = 5.81$	$\omega_{min.} = -5.2628; \omega_{max.} = 5.2628$
0.07	$\psi_{min.} = -0.035; \psi_{max.} = 0.035$           $\psi_{min.} = -0.035; \psi_{max.} = 0.035$				
	$\omega_{min.} = -4.3390; \omega_{max.} = 4.3390$	$\omega_{min.} = -5.4255; \omega_{max.} = 5.4255$	$\omega_{min.} = -7.7619; \omega_{max.} = 7.7619$	$\omega_{min.} = -8.1148; \omega_{max.} = 8.1148$	
0.09	$\psi_{min.} = -0.045; \psi_{max.} = 0.045$           $\psi_{min.} = -0.045; \psi_{max.} = 0.045$				
	$\omega_{min.} = -5.7820; \omega_{max.} = 5.7820$	$\omega_{min.} = -7.5119; \omega_{max.} = 7.5119$	$\omega_{min.} = -10.5943; \omega_{max.} = 10.5943$	$\omega_{min.} = -10.3435; \omega_{max.} = 10.3435$	
0.093	$\psi_{min.} = -0.0465; \psi_{max.} = 0.0465$         $\psi_{min.} = -0.0465; \psi_{max.} = 0.0465$				
	$\omega_{min.} = -6.0063; \omega_{max.} = 6.0063$	$\omega_{min.} = -7.8406; \omega_{max.} = 7.8406$	$\omega_{min.} = -11.0240; \omega_{max.} = 11.0240$	$\omega_{min.} = -10.6165; \omega_{max.} = 10.6165$	
0.7	$\psi_{min.} = -0.35; \psi_{max.} = 0.35$				
	$\omega_{min.} = -77.6189; \omega_{max.} = 77.6189$	$\omega_{min.} = -91.4968; \omega_{max.} = 91.4968$	$\omega_{min.} = -84.1183; \omega_{max.} = 84.1183$		
0.9	$\psi_{min.} = -0.45; \psi_{max.} = 0.45$				
	$\omega_{min.} = -105.9428; \omega_{max.} = 105.9428$	$\omega_{min.} = -117.6699; \omega_{max.} = 117.6699$	$\omega_{min.} = -103.4349; \omega_{max.} = 103.4349$		
0.93	$\psi_{min.} = -0.465; \psi_{max.} = 0.465$				
	$\omega_{min.} = -110.2397; \omega_{max.} = 110.2397$	$\omega_{min.} = -121.4838; \omega_{max.} = 121.4838$	$\omega_{min.} = -106.1645; \omega_{max.} = 106.1645$		

Table 3. Fourth-Order Numerical Values of Stream Function and Vorticity regarding Different Reynolds Numbers and Different Free Stream Velocity Values (Contd)

Free-stream Velocity Values ( $U_\infty$ [m/s])	Reynolds Number ( $Re$ ) Values				
	100	300	1000	10000	20000
1.0	$\psi_{min.} = -0.5; \psi_{max.} = 0.5$ $\omega_{min.} = -120.2892; \omega_{max.} = 120.2892$	$\psi_{min.} = -0.5; \psi_{max.} = 0.5$ $\omega_{min.} = -188.5509; \omega_{max.} = 188.5509$			
2.0	$\psi_{min.} = -1.0; \psi_{max.} = 1.0$ $\omega_{min.} = -261.002; \omega_{max.} = 261.002$	$\psi_{min.} = -1.0; \psi_{max.} = 1.0$ $\omega_{min.} = -245.4223; \omega_{max.} = 245.4223$			
2.29	$\psi_{min.} = -1.145; \psi_{max.} = 1.145$ $\omega_{min.} = -299.7956; \omega_{max.} = 299.7956$	$\psi_{min.} = -1.145; \psi_{max.} = 1.145$ $\omega_{min.} = -275.9508; \omega_{max.} = 275.9508$			
7.0	$\psi_{min.} = -3.5; \psi_{max.} = 3.5$ $\omega_{min.} = -841.1827; \omega_{max.} = 841.1827$				
9.0	$\psi_{min.} = -4.5; \psi_{max.} = 4.5$ $\omega_{min.} = -1.0343 \times 10^3; \omega_{max.} = 1.0343 \times 10^3$				
9.3	$\psi_{min.} = -4.65; \psi_{max.} = 4.65$ $\omega_{min.} = -1.0616 \times 10^3; \omega_{max.} = 1.0616 \times 10^3$				

Table 4. Second-Order Numerical Values of Stream Function and Vorticity regarding Different Reynolds Numbers and Different Free-stream Velocity Values

Free-stream Velocity Values ( $U_\infty$ [m/s])	Reynolds Number ( $Re$ ) Values				
	100	300	1000	10000	20000
0.02	$\psi_{min.} = -0.01; \psi_{max.} = 0.01$             $\psi_{min.} = -0.01; \psi_{max.} = 0.01$				
	$\omega_{min.} = -1.3421; \omega_{max.} = 1.3421$	$\omega_{min.} = -1.4406; \omega_{max.} = 1.4406$	$\omega_{min.} = -1.8048; \omega_{max.} = 1.8048$	$\omega_{min.} = -3.5311; \omega_{max.} = 3.5311$	$\omega_{min.} = -4.0418; \omega_{max.} = 4.0418$
0.04	$\psi_{min.} = -0.02; \psi_{max.} = 0.02$             $\psi_{min.} = -0.02; \psi_{max.} = 0.02$				
	$\omega_{min.} = -2.7807; \omega_{max.} = 2.7807$	$\omega_{min.} = -3.1958; \omega_{max.} = 3.1958$	$\omega_{min.} = -4.4579; \omega_{max.} = 4.4579$	$\omega_{min.} = -8.0836; \omega_{max.} = 8.0836$	
0.046	$\psi_{min.} = -0.023; \psi_{max.} = 0.023$           $\psi_{min.} = -0.023; \psi_{max.} = 0.023$				
	$\omega_{min.} = -3.2321; \omega_{max.} = 3.2321$	$\omega_{min.} = -3.7847; \omega_{max.} = 3.7847$	$\omega_{min.} = -5.3606; \omega_{max.} = 5.3606$	$\omega_{min.} = -9.4972; \omega_{max.} = 9.4972$	
0.07	$\psi_{min.} = -0.035; \psi_{max.} = 0.035$           $\psi_{min.} = -0.035; \psi_{max.} = 0.035$				
	$\omega_{min.} = -5.1321; \omega_{max.} = 5.1321$	$\omega_{min.} = -6.4033; \omega_{max.} = 6.4033$	$\omega_{min.} = -9.3076; \omega_{max.} = 9.3076$	$\omega_{min.} = -15.2009; \omega_{max.} = 15.2009$	
0.09	$\psi_{min.} = -0.045; \psi_{max.} = 0.045$				
	$\omega_{min.} = -6.8335; \omega_{max.} = 6.8335$	$\omega_{min.} = -8.8644; \omega_{max.} = 8.8644$	$\omega_{min.} = -12.9033; \omega_{max.} = 12.9033$		
0.093	$\psi_{min.} = -0.0465; \psi_{max.} = 0.0465$				
	$\omega_{min.} = -7.0980; \omega_{max.} = 7.0980$	$\omega_{min.} = -9.2523; \omega_{max.} = 9.2523$	$\omega_{min.} = -13.4613; \omega_{max.} = 13.4613$		
0.7	$\psi_{min.} = -0.35; \psi_{max.} = 0.35$				
	$\omega_{min.} = -93.0756; \omega_{max.} = 93.0756$	$\omega_{min.} = -124.9483; \omega_{max.} = 124.9483$	$\omega_{min.} = -152.0087; \omega_{max.} = 152.0087$		
0.9	$\psi_{min.} = -0.45; \psi_{max.} = 0.45$	$\psi_{min.} = -0.45; \psi_{max.} = 0.45$			
	$\omega_{min.} = -129.0331; \omega_{max.} = 129.0331$	$\omega_{min.} = -169.4076; \omega_{max.} = 169.4076$			
0.93	$\psi_{min.} = -0.465; \psi_{max.} = 0.465$	$\psi_{min.} = -0.465; \psi_{max.} = 0.465$			
	$\omega_{min.} = -134.6129; \omega_{max.} = 134.6129$	$\omega_{min.} = -176.1969; \omega_{max.} = 176.1969$			

Table 4. Second-Order Numerical Values of Stream Function and Vorticity regarding Different Reynolds Numbers and Different Free-stream Velocity Values (Contd)

Free-stream Velocity Values ( $U_\infty$ [m/s])	Reynolds Number ( $Re$ ) Values				
	100	300	1000	10000	20000
1.0	$\psi_{min.} = -0.5; \psi_{max.} = 0.5$ $\omega_{min.} = -147.7959; \omega_{max.} = 147.7959$	$\psi_{min.} = -0.5; \psi_{max.} = 0.5$ $\omega_{min.} = -192.1368; \omega_{max.} = 192.1368$			
2.0	$\psi_{min.} = -1.0; \psi_{max.} = 1.0$ $\omega_{min.} = -353.1051; \omega_{max.} = 353.1051$	$\psi_{min.} = -1.0; \psi_{max.} = 1.0$ $\omega_{min.} = -427.4245; \omega_{max.} = 427.4245$			
2.29	$\psi_{min.} = -1.145; \psi_{max.} = 1.145$ $\omega_{min.} = -416.5730; \omega_{max.} = 416.5730$	$\psi_{min.} = -1.145; \psi_{max.} = 1.145$ $\omega_{min.} = -496.4174; \omega_{max.} = 496.4174$			
7.0	$\psi_{min.} = -3.5; \psi_{max.} = 3.5$ $\omega_{min.} = -1.5201 \times 10^3; \omega_{max.} = 1.5201 \times 10^3$				
9.0					
9.3					

Table 5. Stream Function Contour Graphics regarding Different Reynolds Numbers and 0.02 Free-stream Velocity Value as a result of Implementing Fourth-Order Numerical Formulation

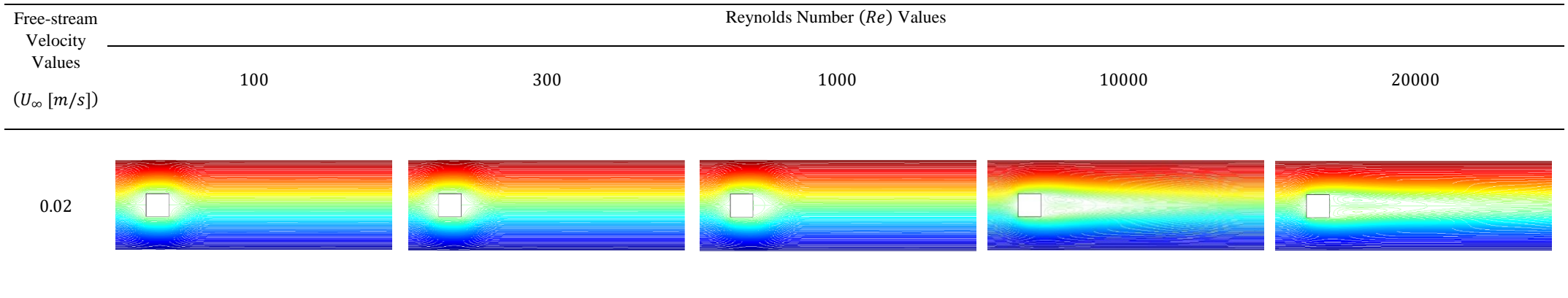
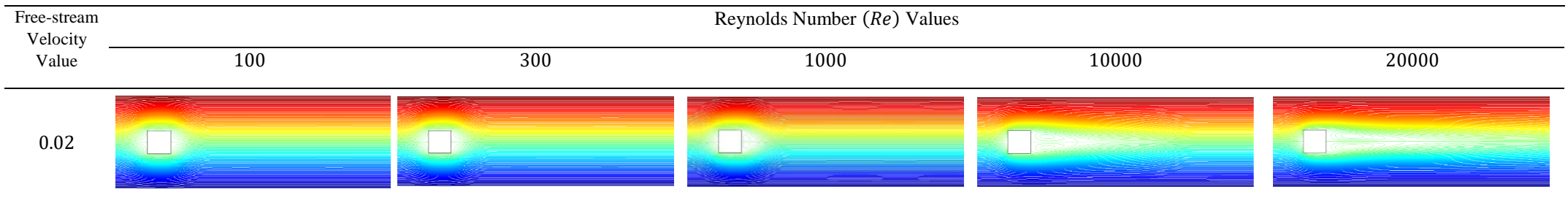


Table 6. Stream Function Contour Graphics regarding Different Reynolds Numbers and 0.02 Free-stream Velocity Value as a result of Implementing Second-Order Numerical Formulation



**Nomenclature**

$A, B, C, D, E$	: Coefficients of used in discretized finite difference equations and iteration equations for stream function and vorticity
$D$	: Any size of square cylinder, [m]
$f$	: In equations general expression of any variable
$H$	: Semi-height of computational domain ( $H = 2D$ ), [m]
$K(x_1, y_1),$ $L(x_1, y_2),$ $M(x_1, y_3)$	: Any grid points in physical or computational domain
$Re$	Reynolds Number ( $= \rho u D / \mu$ ), [-]
$u, v$	Velocity components in $x$ - and $y$ - Cartesian coordinates, respectively
$U$	Velocity, [ $m \cdot s^{-1}$ ]
$x, y$	Two-dimensional Cartesian coordinate directions in physical domain
$X$	: Distance [m]
$w$	: Relaxation parameter

**Greek symbols**

$\beta$	: Blockage ratio
$\Delta h$	: Distance between two sequential grid points in both of $x, y$ or $\xi, \eta$ 2 – $D$ Cartesian coordinates
$\Delta x$	: Distance between two sequential grid points in $x$ -Cartesian coordinate direction for physical domain
$\Delta y$	: Distance between two sequential grid points in $y$ -Cartesian coordinate direction for physical domain
$\Delta \xi$	: Distance between two sequential grid points in $\xi$ -Cartesian coordinate direction for computational domain
$\Delta \eta$	: Distance between two sequential grid points in $\eta$ -Cartesian coordinate direction for computational domain
$\xi, \eta$	: Two-dimensional Cartesian coordinate directions in computational domain
$\lambda$	: Grid stretching parameter
$\nu$	: Kinematic viscosity, [ $m^2 \cdot s^{-1}$ ]
$\psi$	: Stream function
$\psi - \omega$	: Stream function – vorticity
$\omega$	: Vorticity

**Sub- and superscripts**

$i, j$	: Two-dimensional Cartesian coordinate directions in computational domain for $\xi$ and $\eta$ , respectively
<i>downstream</i>	: Flow direction
<i>upstream</i>	: Reverse flow direction
$\infty$	: Free-stream condition

**Acronyms**

<i>ADIM</i>	: Alternating Direction Implicit Method
<i>BEM</i>	: Boundary Element Method
<i>CFD</i>	: Computational Fluid Dynamics
<i>FDM</i>	: Finite Difference Method
<i>FEM</i>	: Finite Element Method
<i>FVM</i>	: Finite Volume Method
<i>LBM</i>	: Lattice Boltzmann Method
<i>N-S</i>	: Navier-Stokes
<i>PDES</i>	: Partial Differential Equation System
<i>TSE</i>	: Taylor Series Expansion

**REFERENCES**

- [1] S. C. Chapra and R. P. Canale “Numerical Methods for Engineers”, 6th edition, McGraw-Hill, Boston, 2010.
- [2] Y. Cengel and J. M. Cimbala, “Fluid Mechanics Fundamentals and Applications (In SI Units)”, McGraw-Hill, Boston, 2006.
- [3] I. Karagoz, “Sayısal Analiz ve Mühendislik Uygulamaları”, 4. Basım, Nobel Akademik Yayıncılık, 2011.
- [4] T. Breuer, J. Bernsdorf, F. Durst, “Accurate computations of the laminar flow past a square cylinder based on two different methods: Lattice-Boltzmann and Finite-Volume”, *Int. J. Heat Fluid Flow*, vol. 21, no. 2, pp. 186-196, 2000.
- [5] M. Ozgoren, “Flow structure in downstream of square and circular cylinders”, *Flow Meas. Inst.*, vol. 17, no. 4, pp. 225-235, 2006.
- [6] C. A. J. Fletcher, “Computational Techniques for Fluid Dynamics I”, Second Edition, Springer-Verlag, Berlin, 1991.

- [7] C. H. K. Williamson, "Vortex dynamics in the cylinder wake", *Ann. Review Fluid Mech.*, vol.28, pp. 477-539, 1996.
- [8] M. M. Zdravkovich, "Flow around Circular Cylinders, vol. 1: Fundamentals", Oxford University Press, New York, 1997.
- [9] A. C. Benim, E. Pasqualotto, S. H. Suh, "Modelling Turbulent Flow Past a Circular Cylinder by RANS, URANS, LES and DES", *Prog. Compt. Fluid Dynamics*, vol. 8, pp. 299-307, 2008.
- [10] R. W. Davis, E.F. Moore, "A numerical study of vortex shedding from rectangles", *J. Fluid Mech.*, vol. 116, pp. 475-506, 1982.
- [11] A. Okajima, "Strouhal numbers of rectangular cylinders", *J. Fluid Mech.*, vol. 123, pp. 379-398, 1982.
- [12] A. Okajima, "Numerical simulation of flow around rectangular cylinders", *J. Wind Eng. Indust. Aerodynamics*, vol. 33, no. 1-2, pp. 171-180, 1990.
- [13] R. W. Davis, E. F. Moore, L. P. Purtell, "A numerical-experimental study of confined flow around rectangular cylinders", *Phys. Fluids*, vol. 27, no. 1, pp. 46-59, 1984.
- [14] R. Franke, W. Rodi, B. Schönung, "Numerical calculation of laminar vortex shedding past cylinders", *J. Wind Eng. Indust. Aerodynamics*, vol. 35, pp. 237-257, 1990.
- [15] K. M. Klekar, S.V. Patankar, "Numerical prediction of vortex shedding behind square cylinders", *Int. J. Numer. Methods Fluids*, vol. 14, no. 3, pp. 327-341, 1992.
- [16] A. Mukhopadhyay, G. Biswas, T. Sundararajan, "Numerical investigation of confined wakes behind a square cylinder in a channel", *Int. J. Numer. Methods Fluids*, vol. 14, no. 12, pp. 1473-1484, 1992.
- [17] A. Sohankar, C. Norberg, L. Davidson, "Numerical Simulation of Flow Past a Square Cylinder", in Proc. 3<sup>rd</sup> ASME/JSME, San Francisco, USA, 1999, pp. 1-6.
- [18] M. Raisee, A. Jafari, H. Babaei, H. Iacovides, "Two-dimensional prediction of time dependent, turbulent flow around a square cylinder confined in a channel", *Int. J. Numer. Methods Fluids*, vol. 62, no. 11, pp. 1232-1263, 2010.
- [19] S. Sen, S. Mittal, G. Biswas, "Flow past a square cylinder at low Reynolds numbers", *Int. J. Numer. Methods Fluids*, vol. 67, no. 9, pp. 1160-1174, 2010.
- [20] T. Bano, N. A. Sheikh, S. Mnazoor, S. Khushnood, "Numerical Simulation of Flow past a Square Cylinder" In Proc. 9th IBCAST, Islamabad, Pakistan, 2012.
- [21] G. Biswas, H. Laschefski, N. K. Mitra and M. Fiebig, "Numerical Investigation of mixed convection heat transfer in a horizontal channel with a built-in square cylinder", *Numer. Heat Trans. Part A*, vol. 18, pp. 173-188, 1990.
- [22] D. Chakrabarty, R. Bharna, "Experimental study of fluid flow and heat transfer from a square prism approaching the wall of a wind tunnel", *J. Eng. Physc. Thermophysics*, vol. 82, pp. 697-705, 2009.
- [23] Y. Yoshida, T. Nomura, "A transient solution method for the finite element method for the finite element incompressible Navier-Stokes equations", *Int. J. Numer. Methods Fluids*, vol. 15, no. 10, pp. 873-890, 1985.
- [24] X. Li, L. Gao, C. Zhang, and X. Shao, "A review on integrated process planning and scheduling," *International Journal of*, vol. 5, no. 2, pp. 161-180, 2010.
- [25] O. Aydın, B. Cuhadaroglu, "Numerical Investigation of Viscous Flow around a Square Obstacle", *Turkish J. Eng. Environmental Sci.*, vol. 21, no. 4, pp. 209-214, 1997.
- [26] E. Erturk, T. Corke, C. Gökçöl, "Numerical solutions of 2-D steady incompressible driven cavity flow at high Reynolds numbers", *Int. J. Numer. Methods Fluids*, vol. 48, no. 7, pp. 747-774, 2005.

- [27] U. Ghia, and R. T. Davis, “Navier Stokes Solutions for Flow Past a Class of Two-Dimensional Semi-Infinite Bodies”, *AIAA Journal*, vol. 12, pp. 1659-1665, 1974.
- [28] A. C. Benim, E. Aslan, I. Taymaz, “Lattice Boltzmann Method for Laminar Forced Convection in a Channel with a Triangular Prism”, *Heat Trans. Res.*, vol. 42, no. 4, pp. 359-377, 2011.
- [29] A. C. Benim, H. Chattopadhyay, A. Nahavandi, “Computational Analysis of Turbulent Forced Convection in a Channel with a Triangular Prism”, *Int. J. Thermal Sci.*, vol. 50, pp. 1973-1983, 2011.
- [30] I. Inan, “Kare Silindir Etrafindan Akan Daimî Sıkıştırılmaz İki-Boyutlu Akışın 4. Hata Mertebesinden Yoğun Formülasyon ile Nümerik Modellenmesi”, MSc. Thesis in Gebze Institute of Technology, 2014.
- [31] E. Erturk, C. Gökçöl, “Fourth-order compact formulation of Navier-Stokes equations and driven cavity flow at high Reynolds numbers”, *Int. J. Numer. Methods Fluids*, vol. 50, no. 4, pp. 421-436, 2006.
- [32] E. Erturk, “Numerical performance of compact fourth-order formulation of the Navier-Stokes equations”, *Commun. Numer. Methods Eng.*, vol. 24, no. 12, pp. 2003-2019, 2008.
- [33] E. Erturk, “CFD Lecture Notes”, Gebze Institute of Technology, 2009.
- [34] C. Gökçöl, “Kararlı Sıkıştırılmayan Navier-Stokes Denklemlerinin Yüksek Dereceli Sıkı Formülasyon İle Çözümü İçin Bir Yöntem Geliştirme”, MSc. Thesis in Gebze Institute of Technology, 2006.
- [35] MATLAB and Statistics Toolbox Release2010a, The MathWorks Inc., Natick, Massachusetts, United States, 2010.
- [36] Ansys-Fluent, Ansys-Fluent User’s Guide, Ansys Inc., Canonsburg, PA, 2009.